Absolute calibration of null correctors using dual computer-generated holograms

Proteep C.V. Mallik[*a], Rene Zehnder[a], James H. Burge[a], Alexander Poleshchuk[b]

[a]College of Optical Sciences, The University of Arizona, Tucson AZ 85721
[b]Institute of Automation and Electrometry, Russian Academy of Sciences, Prospect ak., Koptyuga, 1, Novosibirsk 630090, Russia

ABSTRACT

There is an increasing need for precision large aspheric optics with small focal ratios for astronomical and space applications. However, testing such optics presents a challenge. Interferometric testing of aspheric surfaces often requires the use of null lenses. Many of these null lenses are tested using a certification computer-generated hologram (CGH) for better error calibration. We present a method that will measure large aspheres to a greater level of accuracy than is presently possible. We use segmented and superposed CGH elements to certify and calibrate null lens errors absolutely to a high degree of accuracy. In such holograms two different phase functions are encoded on the CGH by means of aperture division. One subaperture generates a spherical wavefront that is used to determine the pattern errors of the hologram while the second subaperture reconstructs an aspherical wavefront used to calibrate the wavefront errors of the null lens. This careful calibration process involves the removal of both axisymmetric and non-axisymmetric errors in the null test. Once this is accomplished, the null lens may be used to test the asphere to a high degree of accuracy. Our initial results show that we can test 4-meter class aspheric mirrors to better than 1nm rms surface error. In current experiments we have set a goal of measuring such mirrors to better than 1nm rms surface error.

Keywords: Aspheres, Computer-generated holograms, Interferometry, Null-test, Large mirrors

1. INTRODUCTION

Many optical systems, such as telescopes for space and astronomical applications, use very fast aspheres. New technologies in primary mirror fabrication have enabled large, 8-10m, aperture telescopes [1]. Mechanical, optical and cost considerations favor primary mirrors that are fast aspheres [2]. Many such mirrors have focal ratios of 1 or even faster.

It is a challenge to test large, fast aspheres. There are many new and novel techniques for testing large aspheric mirrors [3, 4]. However, interferometric null testing of these mirrors is the most prevalent method of measurement and characterization [5]. In this paper we present a powerful and novel technique using the basic principles of interferometric null testing. This method involves a cascading test using a null lens and computer-generated holograms (CGHs) [6]. The CGH is used to calibrate and certify the null lens, which in turn is used to measure the aspheric mirror.

CGHs are very powerful optical elements because they can encode a wavefront of any desired shape. Thus, they are very useful in the null test of aspheres [7, 8]. For high-accuracy testing of large aspheres, the errors in the CGH need to be carefully characterized [9]. Current limitations in testing have prevented tests of large aspheric mirrors to better than 8-10nm rms surface error. The detailed method that is the topic of this paper shows how we are able to test such surfaces to better than $\lambda/1000$ rms surface error.

The paper is divided into the following sections. Section 1: Introduction, Section 1.1: Interferometric null testing, Section 1.2: Calibration of null corrector, Section 2: Computer-generated holograms, Section 2.1: Fabrication of CGHs, 2.2: Accuracy of CGHs, 2.3: Design of CGHs, Section 3: Calibration of CGHs, Section 3.1: Calibration of non-axisymmetric errors, Section 3.2: Calibration of axisymmetric errors, Section 4: Absolute testing of aspheres, Section 4.1: Quadrant-CGHs, Section 4.2:

---

[*] mallik@email.arizona.edu and phone: 1 (520) 626-6826

Superposed-CGHs, Section 5: Measurements using quadrant-CGHs, Section 6: Test system for null lens calibration, Section 6.1: Alignment of test stand, and Section 7: Conclusions and future work.

1.1 Interferometric null testing

Accurate testing of aspheric mirrors involves using an interferometer with suitably designed null optics. The null optics is designed to create a wavefront that matches the wavefront of the primary asphere. In the absence of null optics the fringe density at the interferometer image plane can be too large for an accurate wavefront measurement. Figure 1 shows the case for a mild asphere.
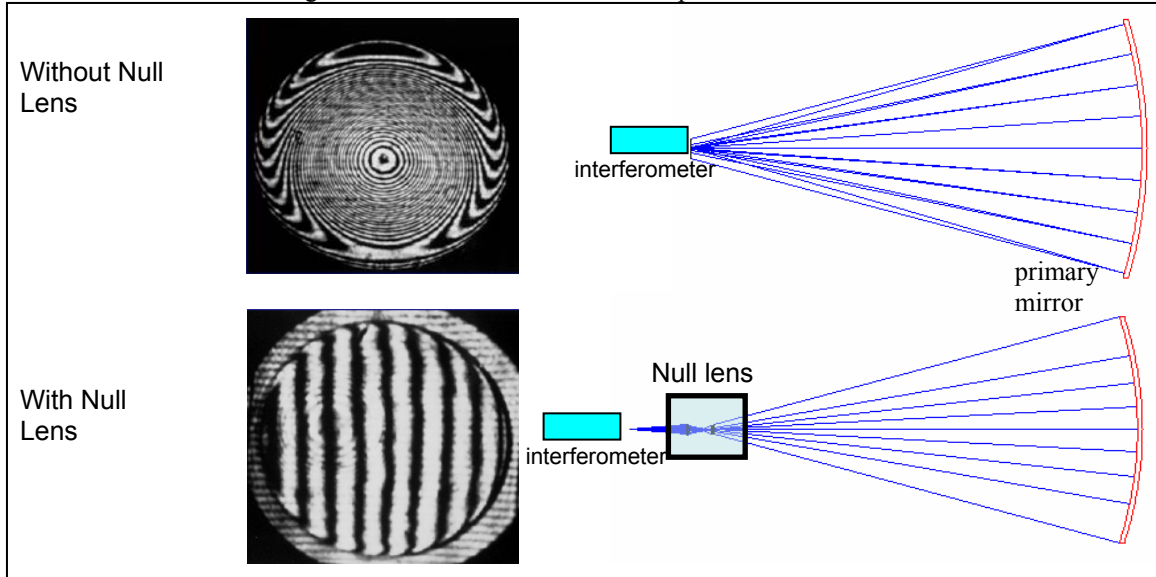

Figure 1: testing a mild asphere without a null lens produces a very high density of fringes at the interferometer image plane. This prevents high accuracy measurements of the aspheric surface. When a suitable null lens is introduced between the interferometer and the asphere, only a few fringes are seen in the image plane, greatly increasing the measurement accuracy.

For the case of steep aspheres the fringes obtained without a null lens is often impossible to resolve, making the measurement almost meaningless.

1.2 Calibration of null corrector

Recent critical errors [10] in testing have made the calibration of null correctors a crucial step. Computer-generated holograms (CGHs) can be effectively used to certify null lenses [3].
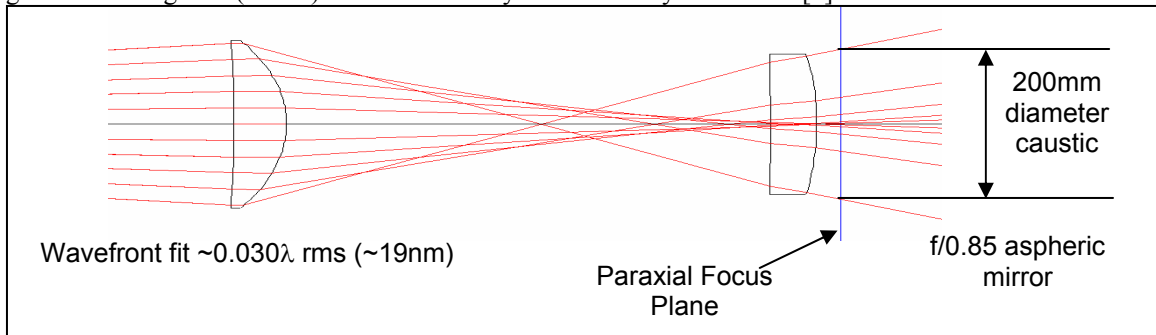

Figure 2: shows a typical Offner null lens design for a 4-meter, f/0.85 parabola. The large residual wavefront from the null corrector needs to be calibrated by a CGH to attain our goal of measuring large surfaces to better than $\lambda/1000$ surface error.

Flaws in the null corrector can result in faulty characterization of the asphere being tested. CGHs can be accurately fabricated and provide an independent reference for measurement of aspheres.

Figure 3 shows the layout for testing an f/0.85 parabola with a diameter of 4-meters. A CGH may directly be used as a null lens [11]. However, for high accuracy testing of aspheres it is more suitable to use a null lens because it has smooth, low order errors. The CGH also causes a very large mapping distortion from the mirror onto the interferometer image plane.

To reach our goal of testing large optics to better than $\lambda/1000$ surface error both a null lens and a certification CGH are needed.

The specifics of how this test is performed are described in the sections to follow. The key concept involves the separation of measurement errors into axisymmetric and non-axisymmetric components.
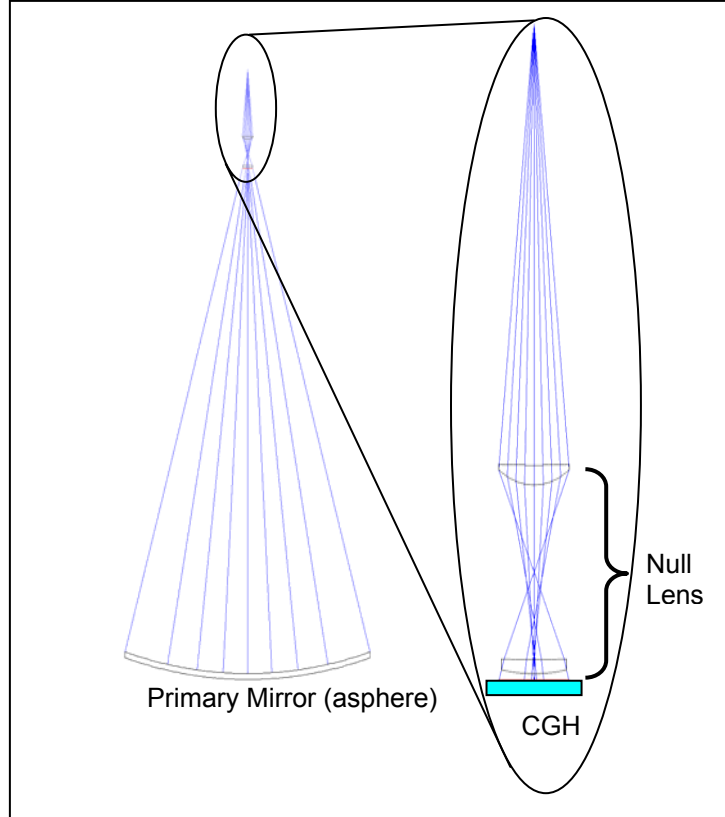

Figure 3: optical layout for an interferometric null test. A blow-up of the null lens setup shows a CGH used to certify the null corrector. The CGH produces a wavefront that mimics the primary mirror under test.

2. COMPUTER-GENERATED HOLOGRAMS

Computer-generated holograms (CGHs) are routinely used in optical testing [8]. They are very powerful elements since a wavefront of any desired shape may be encoded in them.

2.1 Fabrication of CGHs

CGHs may either be phase or amplitude type. For the purposes of this paper we are limiting the discussion to amplitude CGHs.

The amplitude CGHs we use for our measurements are axisymmetric chrome on glass patterns etched by a circular laser writer [12] onto a flat substrate. The CGHs are designed to be used in reflection at a particular order of diffraction. The zero-order diffracted wavefront is used to measure the substrate quality of the CGH.

The CGH writer introduces 2 types of error into the pattern. The first is a spoke-like pattern that comes from the wobble of the writer table. The second is a radial error caused due to axial run out error in the writing head. The wavefront errors, ΔW, from a CGH can be expressed in terms of (r,θ) in the following way:
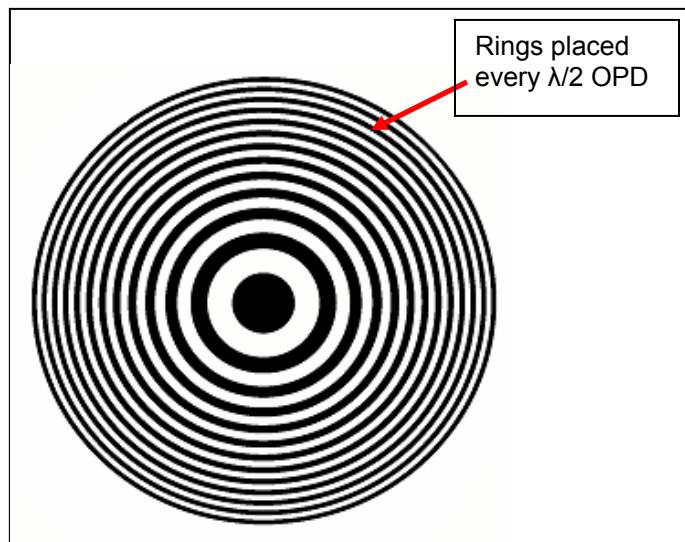

Figure 4: a typical CGH pattern with axisymmetric rings etched every $\lambda/2$ OPD to create an aspheric wavefront.

$$\Delta W(r,\theta) = -m\lambda \frac{\Delta r(r,\theta)}{S(r)} \tag{1}$$

where m is the diffracted order
  λ is the wavelength of light
  Δr is the radial or ring position error
 and S is the CGH line spacing at the given order m

The source of the non-axisymmetric and axisymmetric errors is in the writing process. Figure 5 shows the results from a real measured 60mm diameter CGH. The spoke-like pattern from table wobble can be clearly seen in a) and the axisymmetric component caused by a position error in the writing head can be seen in b).

2.2 Accuracy of CGHs

CGHs can be fabricated to have very high accuracy. Typically, CGHs fabricated with the circular laser writer calibrates the as-built system to about 6nm rms accuracy. The null lens, which corrects for aspheric departure, has about 0.03λ or 18nm rms residual error. CGHs have been used as the "gold standard" for several mirrors fabricated at the University of Arizona, including the 2 8.4-meter, f/1.1 LBT primaries, 4 6.5-meter, f/1.25 mirrors, 3 3.5-meter, f/1.5-f/1.75 mirrors and many other smaller ones.
  Table 1 shows the typical accuracy of a CGH to be used to test a 4.3-meter, f/2 near-parabolic mirror at the University of Arizona.
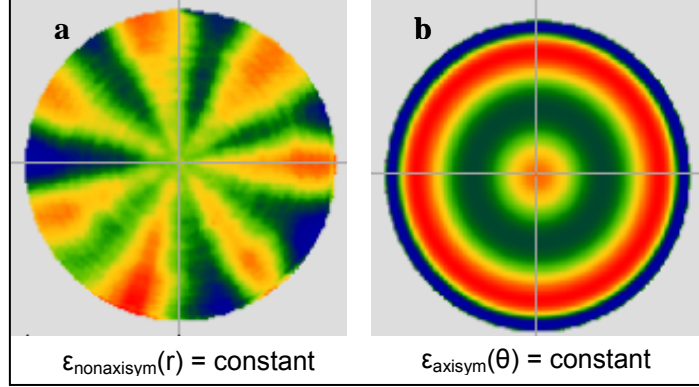

Figure 5: fabrication errors in CGH. a). table wobble causes a non-axisymmetric error constant with r that looks like spokes. b). radial position error of the CGH writer head causes an axisymmetric error constant with θ.
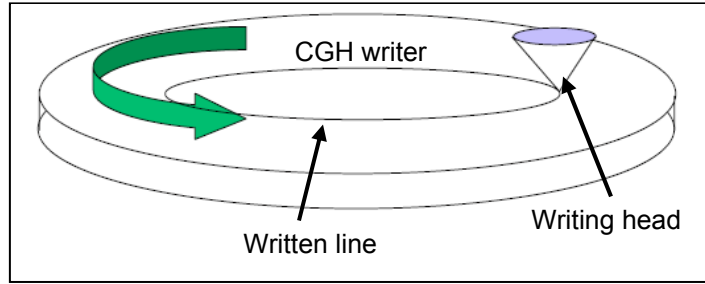

Figure 6: schematic of the circular CGH writer showing a rotating table and fixed laser writer head.

Error Term	Value	dK (ppm)	SA (nm rms)	Figure (nm rms)
Hologram distortion (µm scale)	0.2	21	0.9	
Hologram distortion (µm rms)	0.03			2.6
Substrate figure (rms waves)	0.005			3.2
Chrome thickness variation (nm rms)	2			2.0
Wavelength (ppm)	10	32	1.4	
RSS		**38**	**1.7**	**4.6**

Table 1: shows the accuracy of a CGH design to test a 4.3-meter, f/2 near-parabolic mirror. The final mirror figure error to be achieved is 4.6nm rms. Spherical aberration and the conic constant of the mirror will be measured to better than 2nm rms and 38ppm respectively

2.3 Design of CGHs

As an example, the design for a 220mm diameter CGH for testing a 4-meter f/0.85 parabola is given in this section. Details of how to design CGHs for optical testing are given in [7, 11]. The design of the CGH depends only on the wavefront generated by the aspheric mirror being tested. A specific phase function is encoded onto the CGH. For use in the mth order the CGH will have one plotted fringe for every m waves of OPD. Since this CGH is used in reflection the OPD the phase function must be twice the OPD given above. This gives ring positions for every m X $\lambda/2$ of OPD.
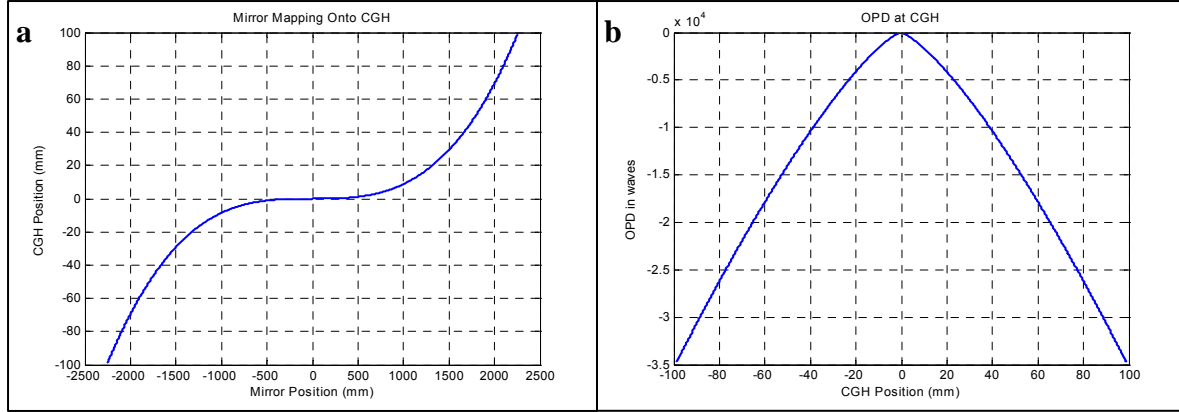

Figure 7: a). The mapping function of the mirror onto the CGH is shown. It is non-linear and is described by equation 2. b). the wavefront (OPD) created at the CGH takes this form and is shown in equation 3.

For a hologram at paraxial focus the rays from the mirror map onto the CGH according to (see figure 7a):

$$x(r) \cong \frac{-Kr^3}{2R^2} \tag{2}$$

The wavefront phase required of a CGH at paraxial focus is described by (see figure 7b):

$$OPD \cong \frac{-3Kr^4}{8R^3} \tag{3}$$

where K is the conic constant of the asphere
 R is the vertex radius of curvature of the asphere
 x(r) is the position on the CGH as a function of ray position on the asphere
 and r is the radial position on the asphere

The spacing of lines on the CGH is shown in figure 8. In later sections a special kind of CGH will be discussed where both aspherical and spherical patterns are encoded into the CGH substrate. In these holograms the radius of curvature of the encoded spherical wavefront is chosen such that the 2 patterns have the same line spacing at the edge of the CGH.
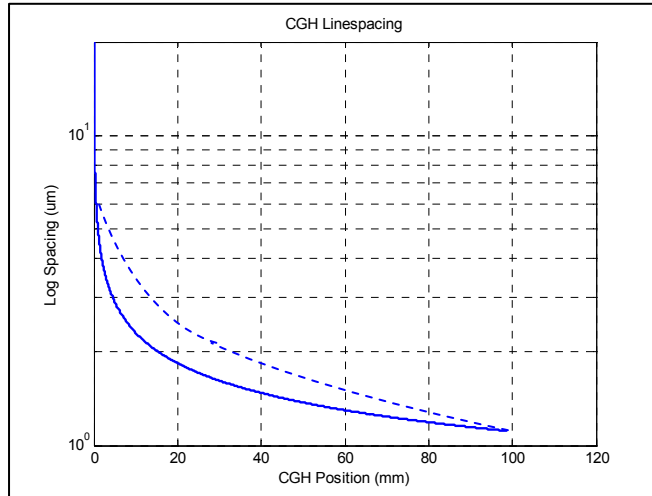

Figure 8: the solid line shows the line spacing as a function of radial position on CGH for an aspheric wavefront. The dashed line shows the line spacing for a CGH designed to create a spherical wavefront

3. CALIBRATION OF COMPUTER-GENERATED HOLOGRAMS

To calibrate the errors in a CGH carefully it is necessary to categorize the types of errors into axisymmetric and non-axisymmetric components. Figure 9 shows a chart labeling the types of CGH errors. The axisymmetric errors in a CGH are due to both pattern distortion and substrate errors. The non-axisymmetric component is due to the non-axisymmetric part of the substrate error.

Dividing the errors into pattern distortion and substrate errors we show how each of them can be divided up into axisymmetric and non-axisymmetric components. The non-axisymmetric errors can be calibrated by the N position test [13]. What remains are the axisymmetric errors. The axisymmetric errors can be found by analyzing the wavefront from the 1st diffracted order, details of which are given in section 5. Figure 10 below shows an example measurement of a 60mm diameter CGH in both the 1st order and 0 order. The measurement in each order can be divided into axisymmetric and non-axisymmetric components.
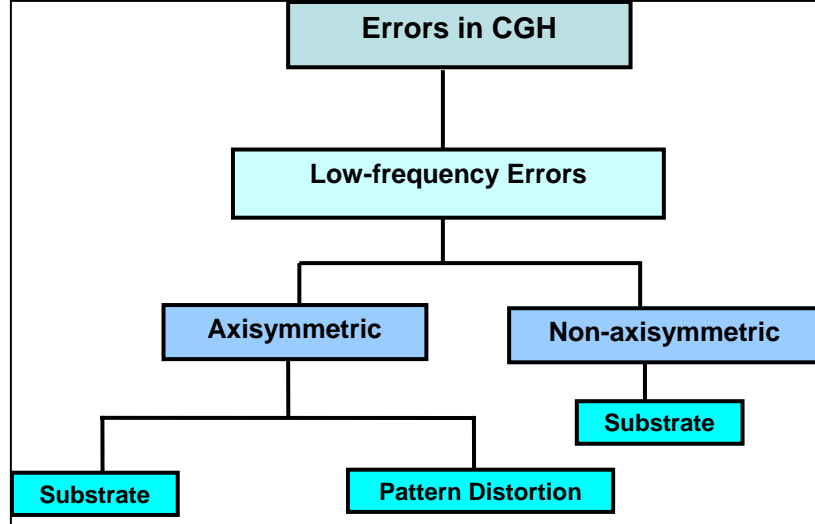

Figure 9: chart showing the categorization of the types of low frequency errors present in a CGH.
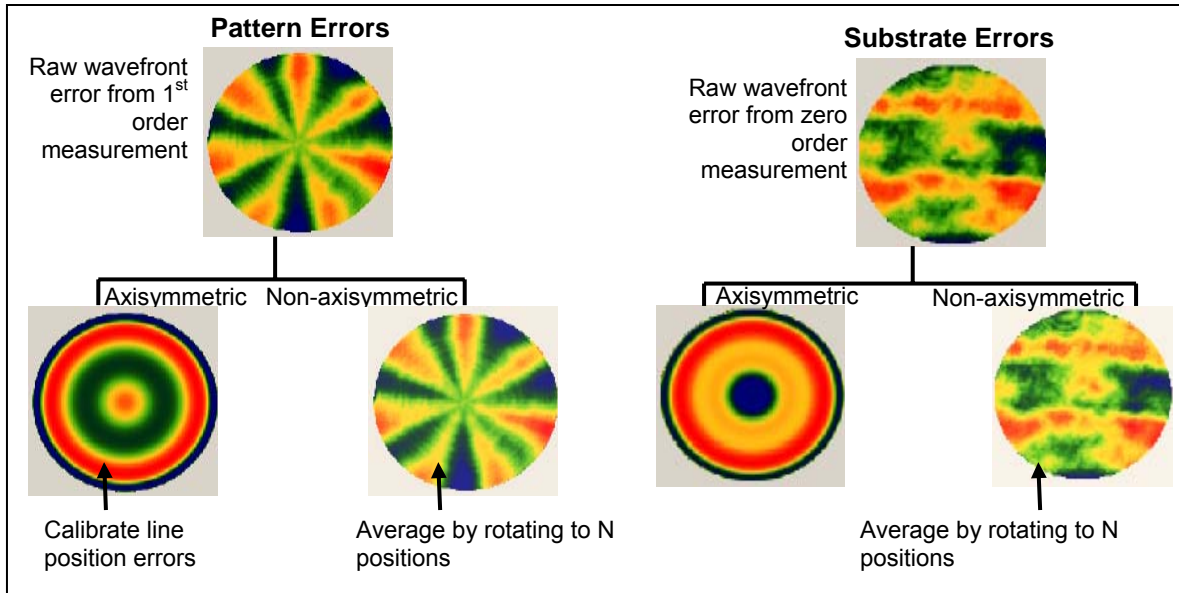

Figure 10: shows the basic break-up of pattern and substrate errors into both axisymmetric and non-axisymmetric components.

3.1 Calibration of non-axisymmetric errors

Evans and Kestner [13] have shown how to calibrate axisymmetric and non-axisymmetric errors in an optical test system. The technique they use is based on the powerful N-position test. Rotating the CGH to N equally separated azimuthal positions, where $N\theta = 360^0$, removes all errors non-axisymmetric errors

excepting harmonics of Nθ, i.e., errors of the form kNθ where k = 1, 2, 3… . The residual error is axisymmetric error.

For example, a 1θ dependent error such as coma can be removed by rotating the test part by 180^0 (N = 2). However, it can be easily seen that a 2θ dependent error such as astigmatism is unaffected by averaging 2 such measurements. Taking a more complex example, the figure below shows a wavefront simulated with error terms up to 5θ. Rotating the wavefront map by 3 equal positions and averaging removes all errors except the 3θ term.
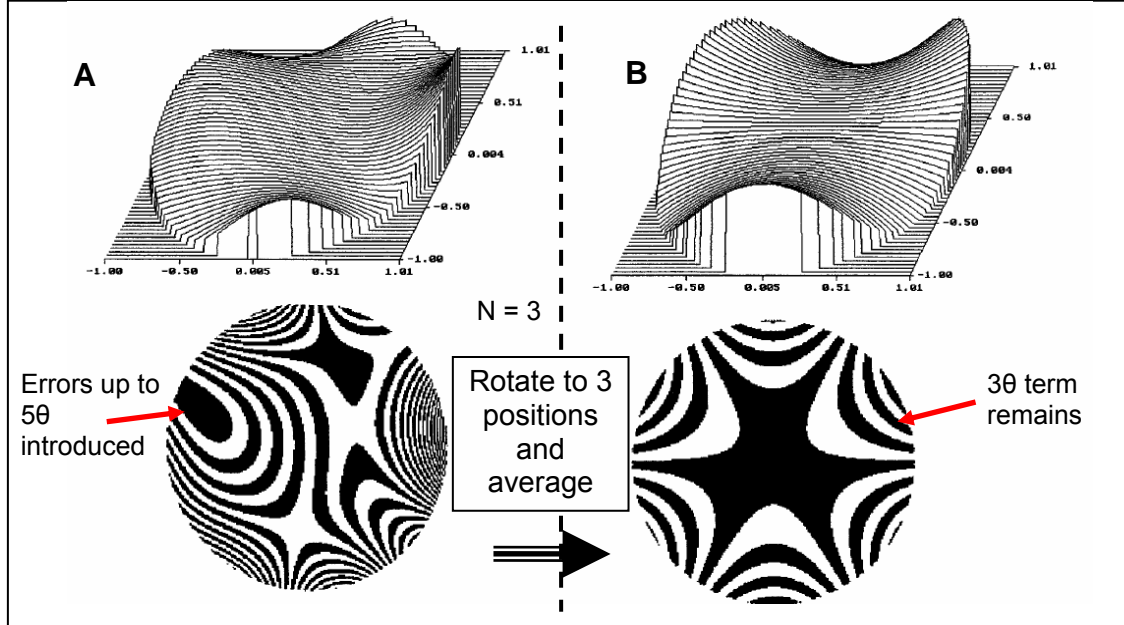

Figure 11: A). A wavefront map is simulated with error terms up to 5θ. B). When rotated by 3 equal positions all error terms average out excepting the error term with a 3θ dependence.

3.2 Calibration of axisymmetric errors

The calibration of axisymmetric errors involves measuring the CGH in the 1st diffracted order and analyzing the wavefront. From the analyzed wavefront the line spacing errors can be calculated. Software has been developed by the authors to perform this calculation from a measured wavefront. The calculation steps include: 1. Making a wavefront measurement, 2. Rescaling the data by correcting for distortion, 3. Calculating the CGH line spacing, 4. Comparing this line spacing with the designed line spacing to give the spacing error.
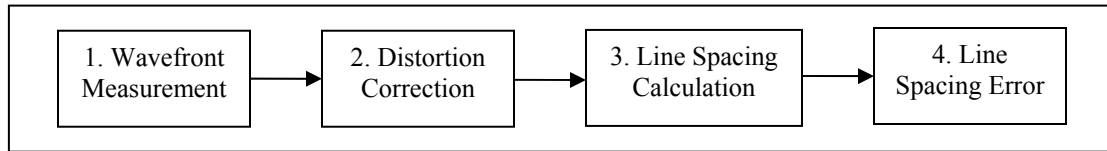

Figure 12: the calculation flowchart for measuring axisymmetric errors in a CGH.

3.2.1 Distortion correction

The non-linear mapping of mirror coordinated onto the CGH leads to distortion or scale error. This can easily be seen when viewing a footprint diagram in the optical design model of a CGH null certification test. The mapping of coordinates obeys the following form:

$$x' \to \rho \to a.\rho^3$$
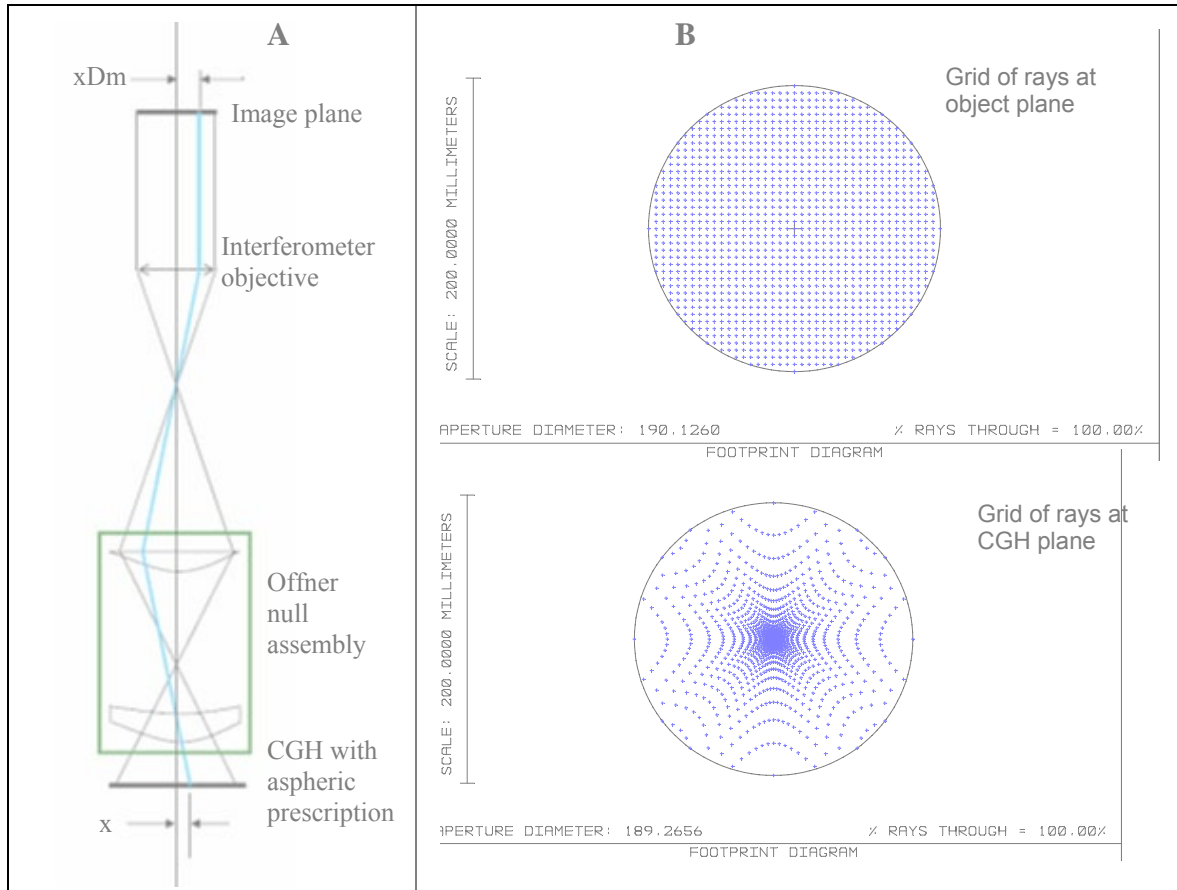$$y' \to \theta \to \theta'$$

(4)

Figure 13: A). Shows the mapping distortion. B). A grid of rays at the object plane and at the CGH plane showing the large mapping distortion.

Figure 13A above shows how the CGH maps onto the image plane with distortion. D is the distortion mapping function. Figure 13B shows a grid of rays at the object plane and the same set of rays at the CGH (image) plane. The distortion correction does not change the amplitude of the wavefront error.

Section 4 describes how the line spacing errors are calibrated for CGHs, in particular for special kinds of CGH that are called dual-CGHs.

4. ABSOLUTE TESTING OF ASPHERES

A method for absolute interferometric testing of axially symmetric aspheres has been devised by Reichelt et al [14]. This method involves the use of a specially designed CGH that reconstructs both the aspherical and spherical auxiliary waves. Such a CGH is referred to as a dual-CGH. The dual-CGH used in our measurements is segmented into 4 quadrants as shown in figure 14. The spherical and aspherical patterns are encoded onto the CGH simultaneously, and thus the errors in the spherical pattern can be transferred to the aspherical pattern directly. The errors in the spherical pattern are measured absolutely [15]. Another type of dual-CGH is the superposed CGH, where the 2 patterns are summed and encoded onto the CGH substrate. In this case the pattern is spatially superposed and not divided up into distinct apertures.

4.1 Quadrant CGHs

The quadrant CGHs used in our measurements consist of 4 segments, 2 of which produce an aspherical wavefront and the other 2 produce a spherical wavefront. The spherical quadrants can be measured absolutely using the 3-position test for spheres [16].

The error calibration steps for such a hologram are shown below in figure 15. First the wavefront errors in the sphere are measured. This multiplied by the line spacing for the spherical part of the encoded pattern gives the line spacing errors in the spherical quadrants (scaled by the wavelength of light). Since both patterns are written at the same time, these

Figure 14: the quadrant CGH is schematically shown with aspherical and spherical patterns encoded by means of aperture division.

line spacing errors are the same in the case for the aspherical patterns. The aspherical line spacing error divided by the line spacing for the aspherical pattern gives the wavefront errors in the encoded asphere (scaled by the wavelength).
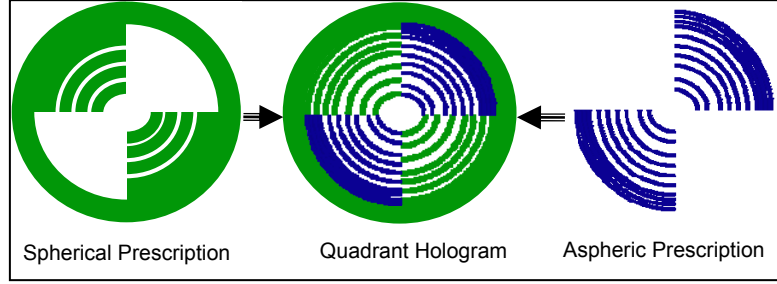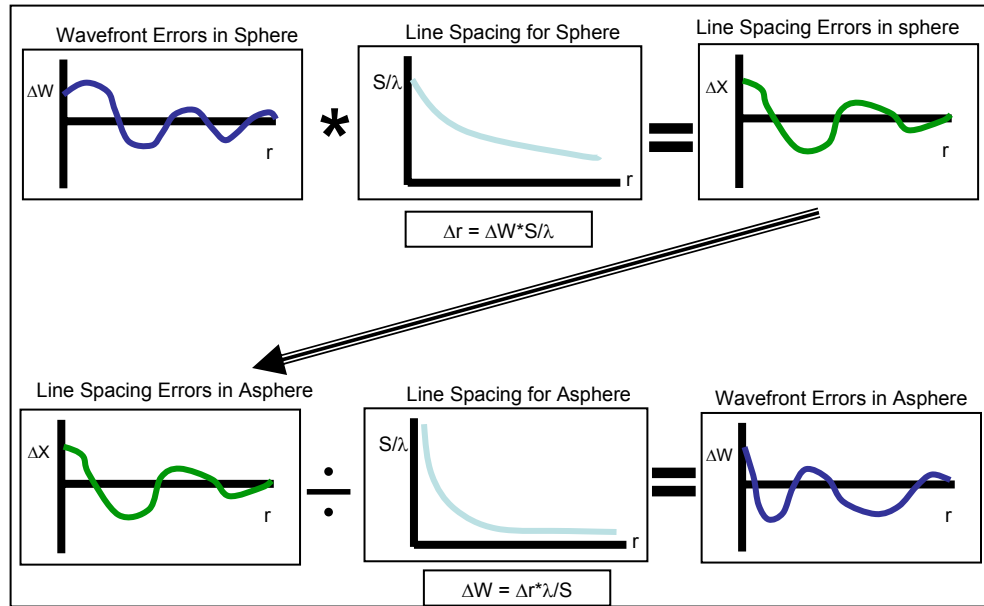

Figure 15: the steps for the absolute calibration of an aspheric CGH is schematically shown.

4.2 Superposed CGHs

Another form of a dual CGH is achieved by superimposing the spherical and aspherical patterns and encoding the resulting pattern onto the whole CGH substrate.

    A preliminary 1-D design for such a CGH is described. This type of CGH will be used to perform the null test of the Discovery Channel's 4.3-meter telescope primary mirror [17].

Figure 16: shows a schematic for a superposed CGH pattern with spherical and aspherical prescription

The spherical and aspherical parts of the superposed CGH can be treated as 2 binary functions with complex amplitude and phase [18]. The complex amplitudes, U_1 and U_2, of each function add according to:

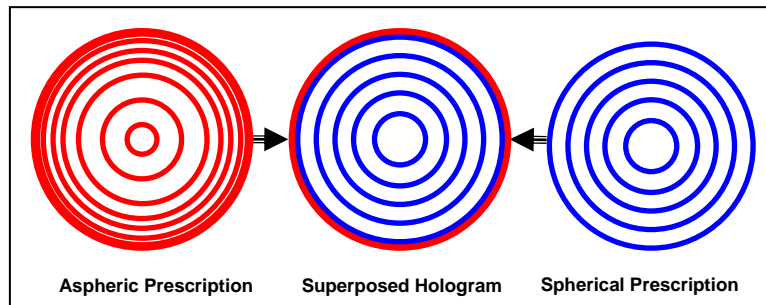$$U_R = U_1 + U_2 = A_1 e^{i\varphi_1} + A_2 e^{i\varphi_2}$$

(5)

where the amplitude, A_R, can be written as:

$$A_R = \left[\left(\mathrm{Re}\{U_R\} \right)^2 + \left(\mathrm{Im}\{U_R\} \right)^2 \right]^{1/2}$$

(6)

and the phase, Φ_R, can be expressed as:

$$\Phi_R = \arctan \left[\frac{\mathrm{Im}\{U_R\}}{\mathrm{Re}\{U_R\}} \right]$$
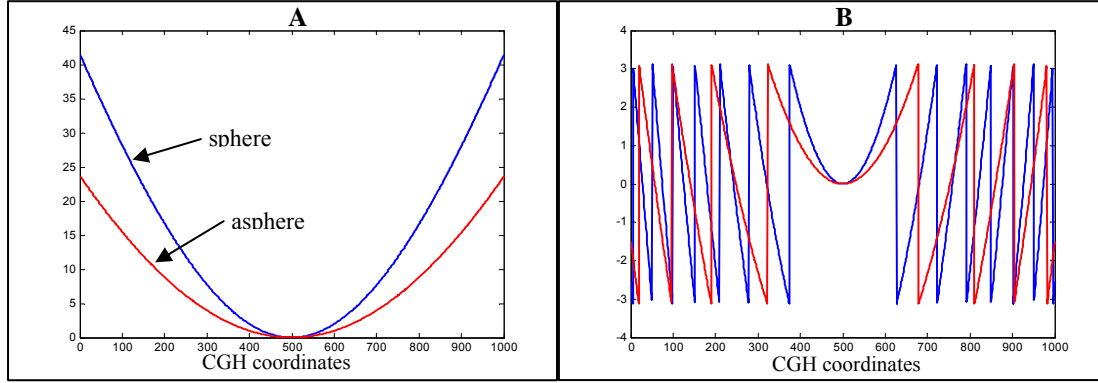
(7)

Figure 17: a). the OPD and b). the unwrapped OPD in radians for the sphere and asphere are shown. The scale on the axes is arbitrary.

Figure 17 a) shows the wavefront OPD from a sphere and an asphere. Taking the unwrapped OPD shown in figure 17 b) and summing the phases as shown in eq. 5 we find that the resulting 1-D binary pattern looks like that shown in figure 18.

The design does not, as of yet, address the issues of crosstalk between the various orders of diffraction or the limitations of the minimum line width that can be etched with a circular laser writer.
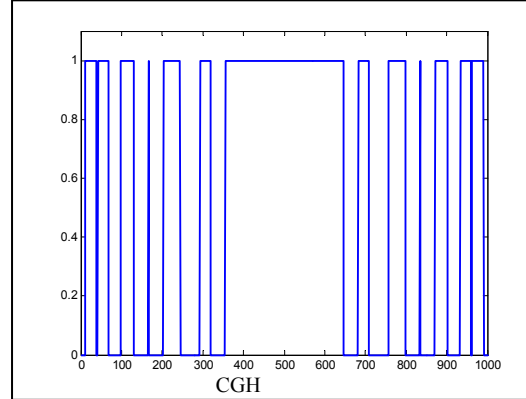

Figure 18: superposed 1-D pattern of a sphere and asphere. The scale is arbitrary.

5. MEASUREMENTS USING QUADRANT CGH

Two prototype quadrant CGHs were fabricated and the quadrants with the spherical prescription were tested. These quadrant CGHs are 35mm in diameter, with a wavefront RoC of 67mm and 59mm. The wavefronts from the spherical quadrants of the 2 CGHs tested are shown in figure 19. Below the wavefront map corresponding to each CGH is the surface error followed by the line spacing error. The CGH line spacing is obtained from calculations using the test wavefronts and compared with the line spacing specified in the design.

The results from our initial tests are very encouraging. The CGH line position errors are less than 10nm rms. This results in corresponding CGH surface errors of about 1nm rms. This is very close to our goal of measuring these errors to the $\lambda/1000$ level. Figure 20 shows the large CGH designed to test a 4-meter f/0.85 parabola. The substrate quality is excellent as seen in figure 21.
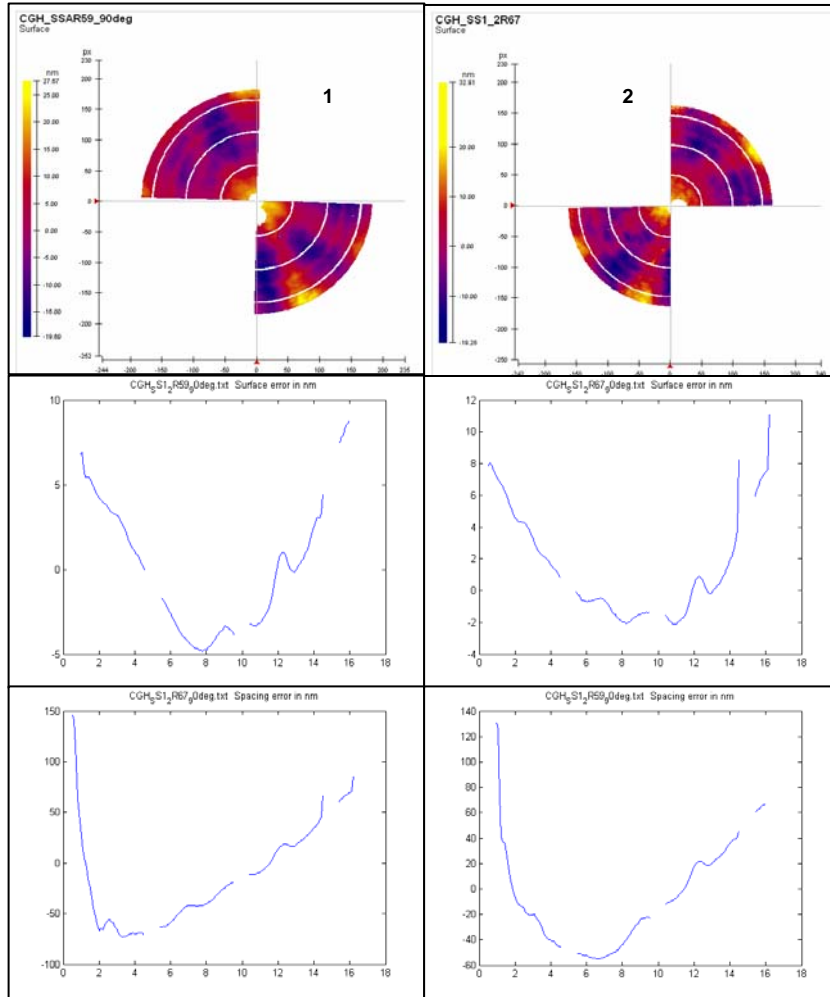
Figure 19: the measurements from 2 prototype CGHs are shown. CGH 1 and CGH 2 are sphere-asphere quadrant CGHs with spherical RoCs of 59mm and 67mm respectively. The surface error and line spacing error for each CGH is given below the corresponding wavefronts.
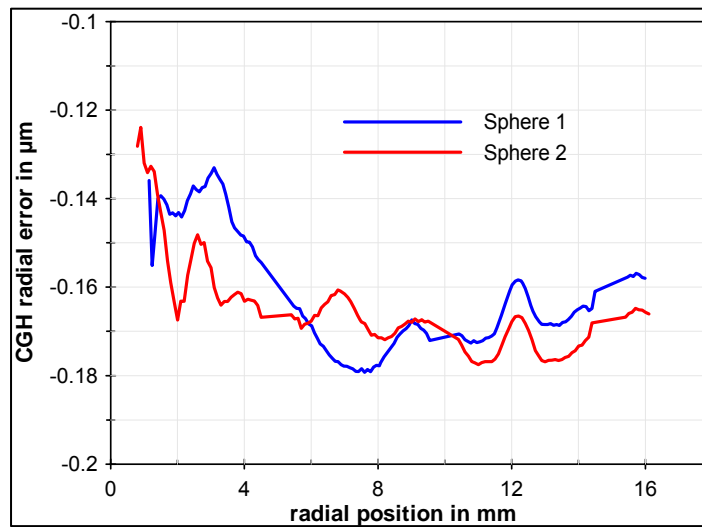

Figure 20: the measured wavefronts show that the CGHs have less than 1nm rms surface error.

Currently measurements of the null lens are being made using the large 220mm diameter CGHs. For the purpose of this test a fully automated test stand has been built and optically aligned.

The substrate quality of the large CGHs is very good. Figure 21 shows a substrate test and a picture of the quadrant CGH.
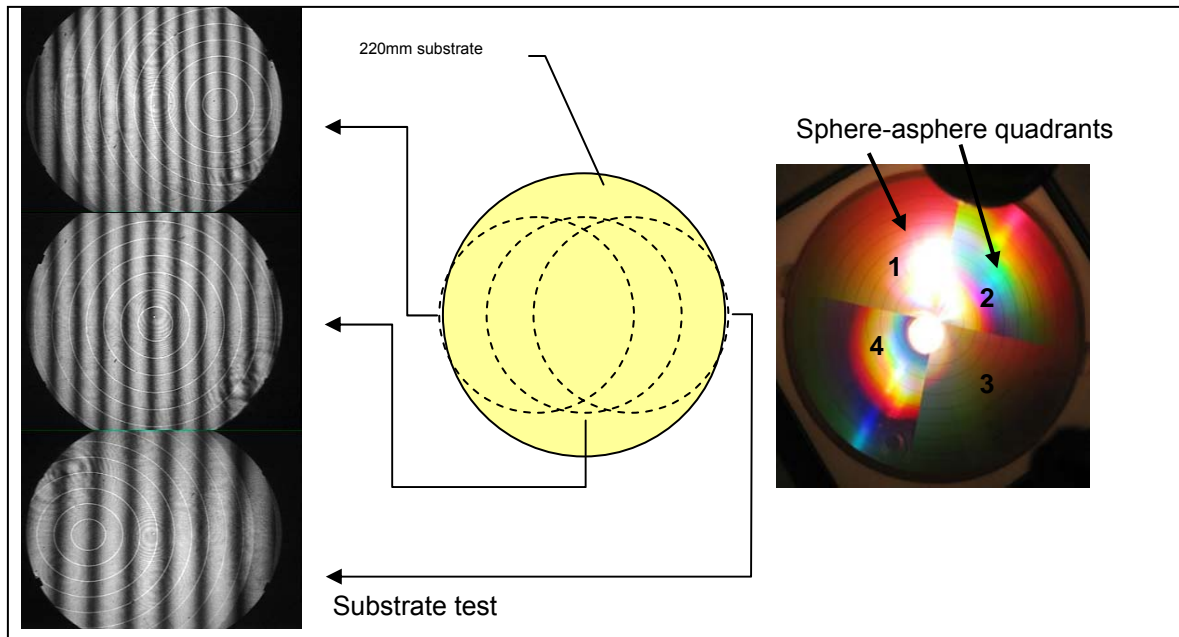

Figure 21: the quadrant CGH showing the substrate quality.

6. TEST SYSTEM FOR NULL LENS CALIBRATION

A test stand to calibrate the null lens with the dual CGHs has been built at the University of Arizona. The test stand is a 7-axis system with automated motion control for the CGH and the interferometer, as shown in figure 22 a) and b).
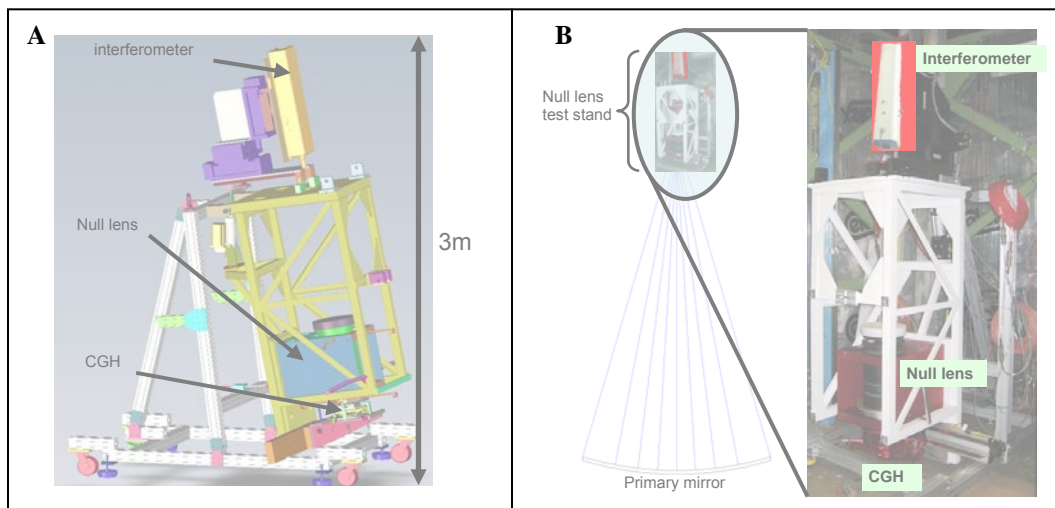

Figure 22: a). a model of test stand for calibrating large null lenses to very high accuracy and b). the built test stand showing an overlay of the final optical layout of the test of a large 4-meter, highly aspheric mirror.

The CGH and the interferometer can each be positioned precisely along their 6 degrees of freedom. The axial positional accuracy for each axis is better than 1μm while the rotational accuracy of the CGH is better

than 1 arcsecond. The precise positioning of the CGH and interferometer enables us to make very accurate measurements of the CGH and the null lens. The basic alignment steps are given in the section 6.1.

6.1 Alignment of test stand

The precise alignment of the null certification test stand is essential to making high accuracy measurements of the CGH and the null lens. Figure 23 shows the test stand on which the alignment schematic is overlaid. The alignment steps consist of the following:
1. Mount the null lens in its cage.
2. Place the spherical alignment mirror with a ~700mm radius of curvature kinematically on the null lens holder. The mirror and null lens have been pre-aligned by the manufacturer.
3. Align the interferometer to the alignment mirror.
4. Remove the alignment mirror. The interferometer is now aligned to the null lens.
5. Align the CGH to the interferometer.
6. Make fine alignment adjustments on the CGH and interferometer to remove residual, high-order spherical aberration.
　　　The above steps have yielded excellent measurements of the CGH so far. This data is currently being analyzed.
　　　The complete alignment is accomplished via a computer interface that has motion control software

Figure 23: shows the alignment schematic for the test stand.

installed. The software interface is user friendly and very easy to modify. Joystick controls have also been implemented for real-time and quick adjustments.
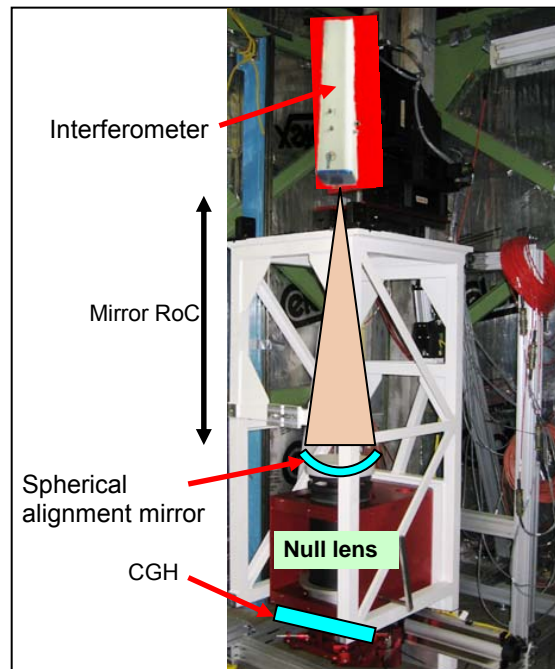
11. CONCLUSIONS AND FUTURE WORK

We have described a cascading test for accurate measurement of large primary aspheric mirrors for astronomical and space applications. This method, proposed by researchers in the recent past, has been implemented by us to measure 4-meter class mirrors in our large optics shop at the University of Arizona. We have shown how accurate calibration of null tests can be accomplished using careful error separation. We use 2 types of special computer-generated holograms (CGHs), quadrant-CGHs and superposed-CGHs, to perform calibrations of null lenses in a systematic manner. We show results of such measurements using small, prototype CGHs.
　　　We are currently testing large, 220mm diameter CGHs, designed for testing 4-meter, f/0.85 parabolas using a test stand with precise automation controls. Our aim is to test the CGHs and the null lenses to better than 1nm rms surface error. This level of accuracy for testing large aspheres has not been achieved in the past. We are currently implementing this test for the 4.3-meter Discovery Channel Telescope primary mirror being polished in the University of Arizona. Analysis has shown that the CGHs for this test can be calibrated to better than 5nm rms surface error.

ACKNOWLEDGEMENTS

REFERENCES

1. J. R. P. Angel, "8-m borosilicate honeycomd mirrors", in ESO Conference on Very Large Telescopes and Their Instrumentation, ed. M. Ulrich, Proc ESO **30**, 281-300 (1988)
2. J. H. Burge and H. M. Martin, "Optical issues for giant telescopes with extremely fast primary mirrors", in Future Giant Telescopes, eds. J. R. P. Angel and R. Gilmozzi, SPIE **4840**, 226-237 (2003)
3. J. E. Greivenkamp et al, "Sub-Nyquist interferometry: implementation and measurement capability", Opt. Eng. 35, **2962** (1996)
4. P. Murphy et al, "Subaperture stitching interferometry for testing mild aspheres", in Interferometry XIII Applications, eds. Erik Novak, Wolfgang Osten, Christophe Gorecki, Proc. SPIE **6293** (2006)
5. J. Burge, "Cerification of null correctors for primary mirrors", in Advanced Optical Testing and Manufacturing IV, ed. Victor Doherty, Proc. SPIE **1994**, 248-59 (1994)
6. P. Mallik et al, "Absolute calibration on null correctors using twin computer-generated holograms", in Interferometry XIII: Techniques and Analysis, eds. K. Creath and J. Schmit, Proc. SPIE **62920H** (2006)
7. J. Wyant and V. Bennett, "Using computer generated holograms to test aspheric wavefronts", Appl. Opt. **11**(12), 2833-39 (1972)
8. J. Burge, "Applications of computer-generated holograms for interferometric measurement of large aspheric optics", in International Conference on Optical Fabrication and Testing, ed. Toshio Kasai, Proc. SPIE **2576**, 258-69 (1995)
9. J. Burge, "A null test for null correctors: error analysis", in Quality and Reliability of Optical Systems, eds. James Bilbro and Robert parks, Proc. SPIE **1993**, 86-97 (1993)
10. L. allen, "The Hubble Space Telescope optical systems failure report", NASA Report (NASA, Washington, D.C., November 1990)
11. J. Burge, "Advanced techniques for measuring primary mirrors for astronomical telescopes", Ph.D. Dissertation, Optical Sciences Center, The University of Arizona, (1993)
12. A. Poleshchuk and V. Korolkov, "Laser writing systems and technologies for fabrication of binary and continuous-relief diffractive optical elements", in International Conference on Lasers, Applications, and Technologies (LAT-2007), Proc. SPIE **6732**, 2007
13. C. Evans and R. Kestner, "Test optics error removal", Appl. Opt. **35**(7), 1015-21 (1996)
14. S. Reichelt et al, "Absolute interferometric test of aspheres by use of twin computer-generated holograms", Appl. Opt. **42**(22), 4468-79 (2003)
15. S. Reichelt et al, "Absolute interferometric test of Fresnel zone plates", Opt. Comm **200**, 107-17 (2001)
16. K. Creath and J. Wyant, "Testing spherical surfaces: a fast, quasi-absolute technique" Appl. Opt. **31**(22), 4350-4354 (1992)
17. M. MacFarlane and E. Dunham, "Optical design of the Discovery Channel Telescope", in Ground-based Telescopes, ed. J. Oschmann, Jr., Proc. SPIE **5489**, 796-804 (2004)
18. S. Reichelt and H. Tiziani, "Twin-CGHs for absolute calibration in wavefront testing interferometry", Opt. Comm. **220**, 23-32 (2003)